Journal of Process Control 58 (2017) 131–138

Contents lists available at ScienceDirect

Journal of Process Control

journal homepage: www.elsevier.com/locate/jprocont

Research paper

Fault detection of process correlation structure using canonical variate analysis-based correlation features

Benben Jiang [a,b,*], Richard D. Braatz [b]

[a] College of Information Science and Technology, Beijing University of Chemical Technology, Beijing 100029, China
[b] Department of Chemical Engineering, Massachusetts Institute of Technology, Cambridge, MA 02139, USA

ARTICLE INFO

Article history:
Received 7 November 2016
Received in revised form 9 August 2017
Accepted 4 September 2017

Keywords:
Fault detection
Process correlations
Dimensionality reduction technique
Canonical variate analysis
Canonical correlation
Process monitoring

ABSTRACT

This paper proposes a canonical variate analysis (CVA) approach based on feature representation of canonical correlation for the monitoring of faults associated with changes in process correlations, which involves two new metrics, R_s and R_r, corresponding to the state and residual spaces. The utilization of the canonical correlation feature can improve the monitoring proficiency by providing more application-dependent representations compared with the original data, as well as a decreased degree of redundancy in the feature space. A physical interpretation is provided for the canonical correlation-based method. The effectiveness of the proposed approach for the monitoring of process correlation changes is demonstrated for both abrupt (step change) and incipient (slow drift) types of faults in simulation studies of a network system. In the simulation results, the canonical correlation-based method has superior performance over both the causal dependency-based method and the traditional variable-based method.

1. Introduction

With the increasing demand for production efficiency, energy savings, and environmental protection, many industrial processes are moving in the direction of large-scale and complicated structures. Industries can face large economic loss and security threats when faults occur. It is important to detect and diagnose abnormal events to improve the reliability and safety of industrial processes by utilizing fault monitoring techniques. A variety of the process monitoring approaches designed so far, such as multivariate statistical control charts [1,2], state-space/time-series approaches [3,4], and dimensionality reduction techniques [5–7], focus on the monitoring of process variables to detect faults [8].

In contrast to the high level of performance achieved in the fault monitoring of process variables, the important complementary problem of monitoring the faults of process correlation structures has not been extensively explored [9]. Process data has grown explosively with the increased scale of manufacturing plants, which represent a valuable resource for the analysis and operations of industrial processes, providing that methods are developed that can effectively extract information from this data. With the rise of the Big Data concept, increasing interest has been raised towards exploiting correlation structures [10]. In sight of these observations, this paper is devoted to developing a new data-driven approach for monitoring changes in process correlations.

Feature representation, which produces derived values (features) from an initial set of data to facilitate the desired task, is of great significance to process monitoring. Sarfraz et al. [11] reported that better fault monitoring results are achieved for features that are more application-dependent. In terms of application-dependence of the feature generation, features that measure the linkages between process variables (e.g., correlation coefficient) are more appropriate than features directly using the process variables themselves for the monitoring of process correlation structures.

The proficiency of monitoring faults from data can be improved using dimensionality reduction techniques such as principal component analysis (PCA) [12,13], partial least-squares (PLS) analysis [14,15], and canonical variate analysis (CVA) [3,16,17]. PCA- and PLS-based monitoring methods are not optimal for the detection of faults for process data that contain significant serial correlation, because the underlying PCA and PLS approaches do not generate the most accurate dynamic models, even when lagged values of process variables are augmented in the observation vectors [3,18,19]. CVA-based approaches [18,19] employ the CVA multivariate system identification method that generates accurate state-space models from serially correlated data. This method maximizes the correlation between the combinations of the "past" values of the process inputs and outputs and the combinations of the "future" values of the outputs of the system. CVA takes serial correlations into account by employing this different augmented vector technique during the dimensionality reduction procedure [18,20]. Negiz and

* Corresponding author at: College of Information Science and Technology, Beijing University of ChemicalTechnology, Beijing 100029, China
E-mail addresses: jiangbb@mail.buct.edu.cn, bbjiang@mit.edu (B. Jiang).

http://dx.doi.org/10.1016/j.jprocont.2017.09.003
0959-1524/

Çinar [3] discuss and demonstrate the higher accuracy of dynamic models constructed by CVA compared to dynamic PCA through application to numerical examples. CVA has been observed to have better numerical stability and parsimony than alternative identification methods, including balanced realization (BR), numerical algorithms for state-space subspace system identification (N4SID), and partial least squares (PLS), in many case studies [4,21].

The maximum correlations produced by the dimensionality reduction procedure of CVA are referred to as *canonical correlations* [18,19,22]. In terms of application dependence of feature representation, canonical correlation is an appropriate feature for monitoring process correlation structures. Canonical correlations are regarded as lower dimensional representations of process dynamic relations. As such, the performance of process monitoring can be enhanced by performing fault detection on the feature space of canonical correlation, owing to the higher sensitivity of the lower dimensional representations of the data [18].

In this article, a new fault detection approach is proposed based on the canonical correlations induced by CVA for the monitoring of process correlations. In virtue of the interpretable correlative levels of canonical correlations, two novel indices, R_s and R_r, that correspond to the state space (that is, retained canonical correlations obtained via CVA) and the residual space (that is, the rest of the canonical correlations in the CVA model) respectively, are put forward to examine the utility of the two different measures for detecting process dynamics. The two types of monitoring statistics (state space and residual space) correspond to different characteristics of the process dynamics and can potentially provide more insights into the fault.

The rest of this paper is organized as follows. The CVA method is briefly reviewed in Section 2, where a geometric interpretation of CVA is also provided. Section 3 presents the canonical correlation-based measures for monitoring correlation structural faults. The effectiveness of the proposed method is demonstrated by a gene network system in Section 4, followed by conclusions in Section 5.

2. Canonical variate analysis (CVA) revisited

2.1. CVA theorem

CVA is a dimensionality reduction technique that aims to maximize a correlation statistic between two sets of variables. Considering the two variable vectors $\boldsymbol{x} \in R^{\mathrm{m}}$ and $\boldsymbol{y} \in R^{\mathrm{n}}$ with covariance matrices $\Sigma_{\boldsymbol{xx}}$ and $\Sigma_{\boldsymbol{yy}}$ and cross-covariance matrix $\Sigma_{\boldsymbol{xy}}$, the orthogonal basis $\boldsymbol{J} \in R^{m\times m}$ and $\boldsymbol{L} \in R^{\mathrm{n}\times \mathrm{n}}$ can be determined from

$$\begin{cases} \boldsymbol{J}\boldsymbol{\Sigma}_{\boldsymbol{xx}}\boldsymbol{J}^{\mathrm{T}} = \boldsymbol{I}_{\tilde{m}} \\ \boldsymbol{L}\boldsymbol{\Sigma}_{\boldsymbol{yy}}\boldsymbol{L}^{\mathrm{T}} = \boldsymbol{I}_{\tilde{n}} \end{cases}, \tag{1}$$

and

$$\boldsymbol{J}\boldsymbol{\Sigma}_{\boldsymbol{xy}}\boldsymbol{L}^{\mathrm{T}} = \boldsymbol{D} = \mathrm{diag}\left(\lambda_1, \cdots, \lambda_r, 0, \cdots, 0\right), \tag{2}$$

where $\tilde{m} = \mathrm{rank}\left(\boldsymbol{\Sigma}_{\boldsymbol{xx}}\right)$, $\tilde{n} = \mathrm{rank}\left(\boldsymbol{\Sigma}_{\boldsymbol{yy}}\right)$, $r = \mathrm{rank}\left(\boldsymbol{\Sigma}_{\boldsymbol{xy}}\right)$, and $\boldsymbol{I}_{\boldsymbol{k}}$ is a block-diagonal matrix with a $k \times k$ identity matrix as the first block and a zero matrix as the second block [18].

The λ_i $(i = 1, 2, \cdots, r)$ are canonical correlations with $\lambda_1 \geq \cdots \geq \lambda_r$ [19]. The vectors of canonical variables $\boldsymbol{c} = \boldsymbol{J}\boldsymbol{x}$ and $\boldsymbol{d} = \boldsymbol{L}\boldsymbol{y}$ contain a set of independent variables with the covariance matrix $\boldsymbol{\Sigma}_{cc} = \boldsymbol{I}_{\tilde{m}}$ and $\boldsymbol{\Sigma}_{dd} = \boldsymbol{I}_{\tilde{n}}$, respectively.

By solving the singular value decomposition (SVD)

$$\boldsymbol{\Sigma}_{\boldsymbol{xx}}^{-1/2}\boldsymbol{\Sigma}_{xy}\boldsymbol{\Sigma}_{\boldsymbol{yy}}^{-1/2} = \boldsymbol{U}\boldsymbol{\Sigma}\boldsymbol{V}^{\mathrm{T}}, \tag{3}$$

the matrix of canonical correlations $\boldsymbol{D}$ can be computed as

$$\boldsymbol{D} = \boldsymbol{\Sigma}, \tag{4}$$

and the projection matrices $\boldsymbol{J}$ and $\boldsymbol{L}$ can be obtained from

$$\begin{cases} \boldsymbol{J} = \boldsymbol{U}^{\mathrm{T}}\boldsymbol{\Sigma}_{\boldsymbol{xx}}^{-1/2} \\ \boldsymbol{L} = \boldsymbol{V}^{\mathrm{T}}\boldsymbol{\Sigma}_{\boldsymbol{yy}}^{-1/2} \end{cases}. \tag{5}$$

The matrices $\boldsymbol{U}^{\mathrm{T}}$ and $\boldsymbol{V}^{\mathrm{T}}$ rotate the canonical variables to be pairwise correlated, and the matrices $\boldsymbol{\Sigma}_{\boldsymbol{xx}}^{-1/2}$ and $\boldsymbol{\Sigma}_{\boldsymbol{yy}}^{-1/2}$ scale the canonical variables to be unit variance.

2.2. CVA algorithm

The CVA method was pioneered by Akaike [23,24]. Larimore [25] both provided a series of later results on and applications of CVA based on state-space representations, and is primarily responsible for convincing the academic and industrial control communities of its value. Given input variables $\boldsymbol{u}(t) \in R^{mu}$ and output variables $\boldsymbol{y}(t) \in R^{my}$, the linear state-space model is formulated as

$$\boldsymbol{x}(t+1) = \boldsymbol{A}\boldsymbol{x}(t) + \boldsymbol{B}\boldsymbol{u}(t) + \boldsymbol{v}(t), \tag{6}$$

$$\boldsymbol{y}(t) = \boldsymbol{C}\boldsymbol{x}(t) + \boldsymbol{D}\boldsymbol{u}(t) + \boldsymbol{E}\boldsymbol{v}(t) + \boldsymbol{w}(t), \tag{7}$$

where $\boldsymbol{A}$,$\boldsymbol{B}$,$\boldsymbol{C}$,$\boldsymbol{D}$, and $\boldsymbol{E}$ are coefficient matrices, $\boldsymbol{x}(t) \in R^d$ is a d-dimensional state vector, and $\boldsymbol{v}(t)$ and $\boldsymbol{w}(t)$ are independent white noise sequences.

The concept of past and future vectors is important to the CVA algorithm. Given a particular time instant t, the past vector comprising of the past outputs and inputs is introduced as

$$\boldsymbol{p}(t) = \left[\boldsymbol{y}_{\mathrm{T}}(t-1), \boldsymbol{y}_{\mathrm{T}}(t-2), \cdots, \boldsymbol{u}_{\mathrm{T}}(t-1), \boldsymbol{u}_{\mathrm{T}}(t-2), \cdots\right]\mathrm{T}, \tag{8}$$

and the future vector containing the outputs in the present and future is defined as

$$\boldsymbol{f}(t) = \left[\boldsymbol{y}_{\mathrm{T}}(t), \boldsymbol{y}_{\mathrm{T}}(t+1), \cdots\right]\mathrm{T}. \tag{9}$$

By substituting the matrix $\Sigma_{\boldsymbol{xy}}$ with $\Sigma_{\boldsymbol{pf}}$, $\Sigma_{\boldsymbol{xx}}$ with $\Sigma_{\boldsymbol{pp}}$, and $\Sigma_{\boldsymbol{yy}}$ with $\Sigma_{\boldsymbol{ff}}$, the matrix of canonical correlations $\boldsymbol{D} = \mathrm{diag}\left(\lambda_1, \cdots, \lambda_r, 0, \cdots, 0\right)$ can be computed via the SVD as (4), and the matrices $\boldsymbol{J}$ and $\boldsymbol{L}$ can be computed as (5). In addition, the canonical variables $\boldsymbol{x}_p(t)$ and $\boldsymbol{x}_f(t)$ which corresponds to the past and future vectors $\boldsymbol{p}(t)$ and $\boldsymbol{f}(t)$ respectively, can be derived as

$$\begin{cases} \boldsymbol{x}_p(t) = \boldsymbol{J}_d\boldsymbol{p}(t) = \boldsymbol{U}_d^{\mathrm{T}}\hat{\boldsymbol{\Sigma}}_{\boldsymbol{pp}}^{-1/2}\boldsymbol{p}(t) \\ \boldsymbol{x}_f(t) = \boldsymbol{L}_d\boldsymbol{f}(t) = \boldsymbol{V}_d^{\mathrm{T}}\hat{\boldsymbol{\Sigma}}_{\boldsymbol{ff}}^{-1/2}\boldsymbol{f}(t) \end{cases}, \tag{10}$$

where $\boldsymbol{J}_d = \boldsymbol{U}_d^{\mathrm{T}}\hat{\boldsymbol{\Sigma}}_{\boldsymbol{pp}}^{-1/2}$ and $\boldsymbol{L}_d = \boldsymbol{V}_d^{\mathrm{T}}\hat{\boldsymbol{\Sigma}}_{\boldsymbol{ff}}^{-1/2}$, and $\boldsymbol{U}_d$ and $\boldsymbol{V}_d$ contains the first d columns of $\boldsymbol{U}$ and $\boldsymbol{V}$ in (3) respectively [18].

Practically, owing to the finite quantity of data available, the vectors $\boldsymbol{p}(t)$ and $\boldsymbol{f}(t)$ are usually truncated to be

$$\boldsymbol{p}(t) = \left[\boldsymbol{y}_{\mathrm{T}}(t-1), \boldsymbol{y}_{\mathrm{T}}(t-2), \cdots, \boldsymbol{y}_{\mathrm{T}}(t-l), \boldsymbol{u}_{\mathrm{T}}(t-1), \boldsymbol{u}_{\mathrm{T}}(t-2), \cdots, \boldsymbol{u}_{\mathrm{T}}(t-l)\right]^{\mathrm{T}}, \tag{11}$$

and

$$\boldsymbol{f}(t) = \left[\boldsymbol{y}_{\mathrm{T}}(t), \boldsymbol{y}_{\mathrm{T}}(t+1), \cdots, \boldsymbol{y}_{\mathrm{T}}(t+h)\right]^{\mathrm{T}}, \tag{12}$$

where l and h are the numbers of lags in vectors $\boldsymbol{p}(t)$ and $\boldsymbol{f}(t)$, respectively. Moreover, the appropriate numbers of lags l and h and the state order d can be determined by the Akaike information criterion [18].

Remark 1. The canonical correlations generated by the CVA algorithm have a geometric interpretation. Calculating $\boldsymbol{J}_d^{(i)}$ and $\boldsymbol{L}_d^{(i)}$ to maximize the correlation between the combinations $\boldsymbol{x}_p^{(i)} = \boldsymbol{J}_d^{(i)}\boldsymbol{p}$ and $\boldsymbol{x}_f^{(i)} = \boldsymbol{L}_d^{(i)}\boldsymbol{f}$—where $\boldsymbol{x}_p^{(i)}$ and $\boldsymbol{x}_f^{(i)}$ are the ith element of canonical variables $\boldsymbol{x}_p$ and $\boldsymbol{x}_f$ respectively, and $\boldsymbol{J}_d^{(i)}$ and $\boldsymbol{L}_d^{(i)}$ denotes the ith row of the projection matrices $\boldsymbol{J}_d$ and $\boldsymbol{L}_d$ respectively—is equivalent to

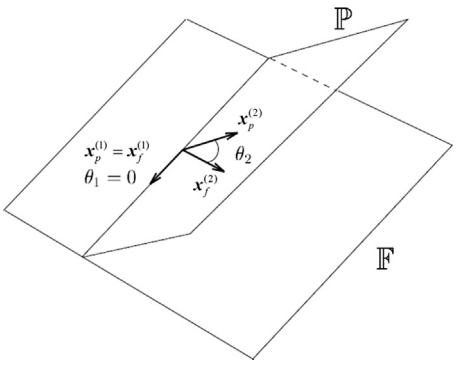

Fig. 1. Interpretation of canonical correlation derived via the CVA algorithm in the i-dimensional space of $\mathbb{P}$ and the j-dimensional space of $\mathbb{F}$ ($i=j=2$ in this case). The vectors $\boldsymbol{x}_p^{(1)} = \boldsymbol{x}_f^{(1)}$ imply the first canonical variables. The angle θ_1 between $\boldsymbol{x}_p^{(1)}$ and $\boldsymbol{x}_f^{(1)}$ is the first minimum angle and $\theta_1 = 0$ in this case. The second minimum angle θ_2 is the angle between the canonical variables $\boldsymbol{x}_p^{(2)}$ and $\boldsymbol{x}_f^{(2)}$, which lie in a plane orthogonal to the intersection of the planes $\mathbb{P}$ and $\mathbb{F}$, since $\boldsymbol{x}_p^{(2)}$ and $\boldsymbol{x}_f^{(2)}$ must be orthogonal to $\boldsymbol{x}_p^{(1)}$ and $\boldsymbol{x}_f^{(1)}$, respectively.

finding the vectors in the space of past data $\mathbb{P}$ and the space of future data$\mathbb{F}$ such that the angle between the vectors is minimum [22]. This selection results in the first canonical variables having the maximum correlation (i.e., the first canonical correlation). Similarly, the second canonical correlation is derived that the second canonical variables correspond to vectors orthogonal to the first canonical variables and with the angle minimized. This procedure is continued in this way until r canonical correlations have been obtained (see Fig. 1).

3. CVA-based correlation measures for monitoring process correlations

Feature representation is crucial for fault monitoring in which derived values (features) are generated from an initial set of data. Features that measure the linkages between process variables (e.g., correlation coefficients) are more appropriate than features directly using the process variables for the monitoring of process correlation structures. In this regard, canonical correlations produced via the augmented vector technique of "past" and "future" data in CVA are appropriate features to represent deviations in the process dynamic relations (which is demonstrated for the case studies in Section 4).

Similar to the traditional CVA-based monitoring method [19], two types of statistics are derived based on the canonical correlations corresponding to the state space (i.e., retained canonical correlations obtained via CVA) and the residual space (i.e., discarded canonical correlations in the CVA model), respectively. The first statistic R_s, which measures the variations of dynamic correlations inside the canonical state space, is defined as

$$R_s = \boldsymbol{\eta}_s^{\mathrm{T}} \boldsymbol{\eta}_s, \tag{13}$$

where $\boldsymbol{\eta}_s = \begin{bmatrix} \lambda_1 & \lambda_2 & \cdots & \lambda_d \end{bmatrix}^{\mathrm{T}}$.

The second statistic R_r, which measures the variations of dynamic relations in the residual space, is defined as

$$R_r = \boldsymbol{\eta}_r^{\mathrm{T}} \boldsymbol{\eta}_r, \tag{14}$$

where $\boldsymbol{\eta}_r = \begin{bmatrix} \lambda_{d+1} & \lambda_{d+2} & \cdots & \lambda_r \end{bmatrix}^{\mathrm{T}}$, and d is the dimensionality reduction order of CVA which can be determined by minimizing the Akaike information criterion [18]. To avoid a particular λ_i from inappropriately dominating the fault detection procedure, canonical correlations $\lambda_i (i = 1, 2, \cdots, r)$ are required to be normalized before the calculation of R_s and R_r in (13) and (14). The statistics R_s and R_r are calculated for a moving window. Whether d is recalculated for each window is a choice by the user; the value of d was fixed in the case studies in Section 4 to minimize online computational cost.

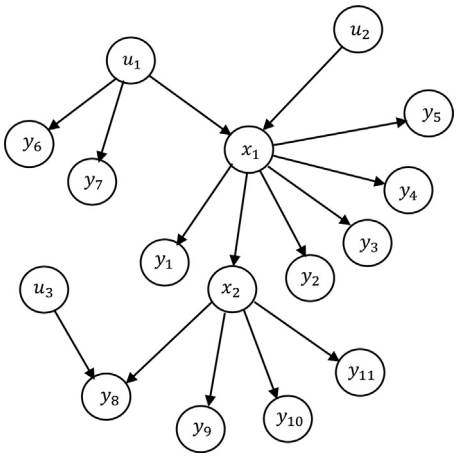

Fig. 2. Causal description of a gene network [30].

The process correlations are regarded as normal if the monitoring metrics are below the thresholds, namely, $R_s \le T_\alpha^2$ and $R_r \le \delta_\alpha^2$, where T_α^2 and δ_α^2 are the upper control limits for the dissimilarity statistic in the state and residual spaces with a significance level α, respectively. In addition, T_α^2 and δ_α^2 can be obtained by using the empirical method based on the calibration samples under normal operating conditions (NOC) [19,26]. For example, a 99% confidence upper control limit can be derived as the R_s or R_r value below which 99% of the calibration data are located.

The portion of the CVA space corresponding to the larger singular values describes most of the *systematic* or *state variations* occurring in the process, and the portion of the CVA space corresponding to the smaller singular values describes the *random noise* [18]. Therefore, a violation of the R_s threshold implies that the process correlations are out of control, whereas a violation of the R_r threshold implies that the characteristic of the process noise has altered.

4. Case studies for a gene network

In this section, a gene network system is utilized to evaluate the proposed canonical correlation-based approach for the monitoring of process correlations, in comparison with causal dependency (CD)-based (i.e., perform CVA on the CDs where the two statistics that measure the variations inside the state and residual spaces are termed as D_s and D_r, respectively) [29], variable-based (i.e., directly perform CVA on the process variables where the two statistics are termed as T_s and T_r) [29], and statistical pattern analysis (SPA)-based (i.e., perform DPCA on the statistical patterns where the two statistics that measure the variations inside the principal and residual spaces are termed as T^2 and Q, respectively) [31,32] methods. In each case study, the normal dataset for training contains 2000 observations; and the testing dataset for each fault also consists of 2000 observations. Each faulty dataset started with no faults, and the faults were triggered after the 1000th observation into the run. The data have a sampling time of one second. A moving window of observation number $N = 500$ is chosen in the step of singular value decomposition (3) in the proposed method.

The proposed canonical correlation-based approach for the monitoring of process correlation faults is evaluated for a gene network adapted from [30], which contains 16 variables causally related according to the description provided in Fig. 2.

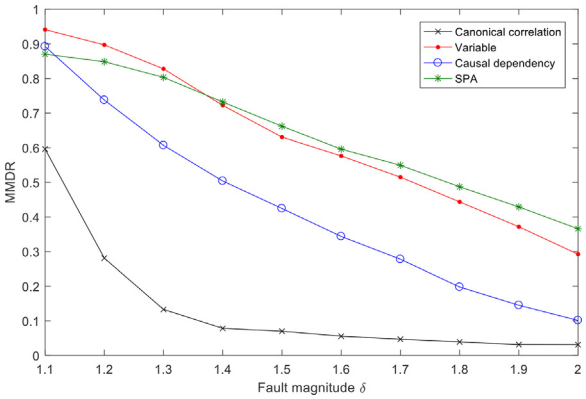

Fig. 3. The mean missed detection rate (MMDR) as a function of the fault magnitude for Fault GN1 ($\delta = 1$ under NOC). The methods in the legend are: Canonical correlation (i.e., the proposed canonical correlation-based method), Causal dependency (i.e., perform CVA on the CDs [29]), Variable (i.e., directly perform CVA on the process variables [29]), and SPA (i.e., perform DPCA on the statistics patterns [31]) methods. For each method, a fault was indicated if either the state or residual statistic violated threshold.

In the case studies, the original variable relationships are linearized according to

$$\begin{cases} x_1(t) = 1.2\,(u_1(t) + 0.60u_1(t-1) + 0.30u_1(t-2)) + 0.8u_2(t) + v_1(t) \\ y_1(t) = 0.60\,(x_1(t) + 0.50x_1(t-1) + 0.20x_1(t-2)) + v_2(t) \\ x_2(t) = 0.05 + 0.22\,(x_1(t) - 0.40x_1(t-1) - 0.20x_1(t-2)) + v_3(t) \\ y_2(t) = 1 + 0.40\,(x_1(t) - 0.20x_1(t-1) - 0.10x_1(t-2)) + v_4(t) \\ y_3(t) = 0.062 + 0.16\,(x_1(t) + 0.40x_1(t-1) + 0.60x_1(t-2)) + v_5(t) \\ y_4(t) = 0.60\,(x_1(t) + 0.80x_1(t-1) + 0.10x_1(t-2)) + v_6(t) \\ y_5(t) = 0.70\,(x_1(t) + 0.40x_1(t-1) + 0.20x_1(t-2)) + v_7(t) \\ y_6(t) = 1 + 0.40\,(u_1(t) + 0.60u_1(t-1) - 0.30u_1(t-2)) + v_8(t) \\ y_7(t) = 0.56 + 0.15\,(u_1(t) + 0.40u_1(t-1) + 0.60u_1(t-2)) + v_9(t) \\ y_8(t) = 0.80\,(u_3(t) + 0.60u_3(t-1) + 0.30u_3(t-2)) + 0.51x_2(t) + v_{10}(t) \\ y_9(t) = 1.30\,(x_2(t) + 0.50x_2(t-1) + 0.50x_2(t-2)) + v_{11}(t) \\ y_{10}(t) = 1 + 0.40\,(x_2(t) + 0.40x_2(t) + 0.60x_2(t)) + v_{12}(t) \\ y_{11}(t) = 0.028 + 1.30\,(x_2(t) + 0.60x_2(t) - 0.30x_2(t)) + v_{13}(t) \end{cases} \quad (15)$$

where u_1, u_2, and u_3 are the input variables, x_1 and x_2 are the states, and the rest are outputs. Each v_i is a white noise sequence with a noise-to-signal ratio of 10%. The system was subject to the two faults (see Table 1), where the type of Fault GN1 is step change and Fault GN2 is a slow drift. For the faults, δ denotes a multiplicative factor that causes a change in a model parameter.

In order to provide meaningful comparisons of the detection performances, the false alarm rates are maintained at the same level ($\alpha = 1\%$) for comparing the missed detection rates throughout this study. The same procedure was repeated 100 times in order to estimate the confidence levels of the missed detection rates at different fault magnitudes.

4.1. Abrupt fault case study

Fault GN1 is a step change fault which occurs in the process structure between input variable u_1 and state variable x_1. For different fault magnitude δ, the mean missed detection rate (MMDR) of Fault GN1 are plotted in Fig. 3 for the canonical correlation-, CD-, SPA-, and variable-based methods.

As the fault magnitude increases, the mean missed detection rate decreases in all of the methods. The mean missed detection rate in all four methods will approach zero as the fault magnitude further increases, indicating the enhanced detectability for large faults. In addition, the mean missed detection rate is fairly sensitive to the fault magnitude for small to intermediate values of δ, and the proposed canonical correlation has the highest sensitivity with regard to the fault magnitude among the four methods.

For the same fault magnitude δ, the canonical correlation-based method consistently outperformed the CD-, variable-, and SPA-based methods (Fig. 3). For instance, for a fault magnitude $\delta = 1.6$, the missed detection rates of the canonical correlation-based algorithm is 5.6%, which is more than a factor of 6.1 and 10.6 improvements compared to the CD-based algorithm (34.4%) and the SPA-based algorithm (59.6%), respectively. Compared with the variable-based algorithm, the mean missed detection rate for the canonical correlation-based algorithm is nearly a factor of 10.3 lower (5.6% vs. 57.6%). There are two major contributors to the superior performance of the canonical correlation-based approach: (*i*) the canonical correlation-based feature representation more effectively captures the changes in the process correlation structures (the application-dependent aspect); and (*ii*) the lower redundancy in the canonical correlation-based feature representation leads to the improved monitoring performance via the dimensionality reduction procedure.

Successful fault detection methods should be *sensitive* enough to detect all possible faults, while also being *robust* to data that are independent of the training set. While the mean missed detection rate (aka type II error [18]) is usually used to quantify the sensitivity for faults in the testing set, the false alarm rate (aka type I error [18]) can help to examine the robustness for the testing set under NOC. The extent to which the methods (with statistics T_s, T_r, D_s, D_r, T^2, Q and R_s, R_r) are sensitive to Fault GN1 is displayed in Fig. 4 with the type I error maintained at the same level ($\alpha = 1\%$) in all methods to enable a fair comparison of the type II errors. A more persistent fault indication is shown in the state statistic R_s for the canonical correlation-based method compared with the other methods.

In summary, the results show that the canonical correlation-based method outperforms the causal dependency-, Statistics Pattern analysis- and variable-based methods, for the monitoring of process correlation structures.

4.2. Incipient fault case study

A slow drift fault (Fault GN2) in the gene network system that occurs in the correlations of $x_1 \to x_2$ is used to further investigate the performance of the proposed approach for monitoring process correlation changes. The mean missed detection rate for different fault magnitude δ values in Fault GN2 with the canonical correlation-, CD-, SPA-, and variable-based methods are plotted in Fig. 5.

Similar to Fault GN1, as the fault magnitude δ increases, the mean missed detection rate of Fault GN2 decreases in all of the methods (Fig. 5). The mean missed detection rates in all four methods also approach zero as the fault magnitude increases, as larger faults would have better detectability. Additionally, the gap in the missed detection rates between the canonical correlation- and CD-based methods enlarges as the magnitude of fault increases from $1 \to 1.2$ to $1 \to 1.6$, while the gap between the canonical correlation- and variable-based/SPA-based methods enlarges as fault magnitude increases from $1 \to 1.1$ to $1 \to 2.0$.

For the same fault magnitude δ, the canonical correlation-based algorithm always provides better fault detection for Fault GN2 than the CD-, SPA- and variable-based algorithms (Fig. 5). For example, for a fault magnitude $\delta = 1 \to 1.3$, the mean missed detection rate for the canonical correlation-based algorithm is more than a factor of 1.5 lower (56.3% vs. 85.8%) than for the CD-based algorithm, nearly a factor of 1.6 for the SPA-based algorithm (56.3% vs. 89.6%), and more than a factor of 1.7 for the variable-based algorithm (56.3% vs. 96.2%). The main reasons are similar to the

Table 1
Definition of the faults and respective variables involved for correlation structures, δ is a multiplicative factor that changes the model parameters ($\delta = 1$ for NOC).

Fault	Process correlation changed	Type
GN1	$u_1 \rightarrow x_1$ $\{x_1(t) = 1.2\delta(u_1(t) + 0.60u_1(t-1) + 0.30u_1(t-2))$ $+0.8u_2(t) + v_1(t)\}$	Abrupt fault: Step change (δ was exerted by a step change after the 1000th sample)
GN2	$x_1 \rightarrow x_2$ $\{x_2(t) = 0.05 + 0.22\delta(x_1(t) - 0.40x_1(t-1)$ $-0.20x_1(t-2)) + v_3(t)\}$	Incipient fault: Slow drift (δ was linearly increased during the samples 1001–2000)

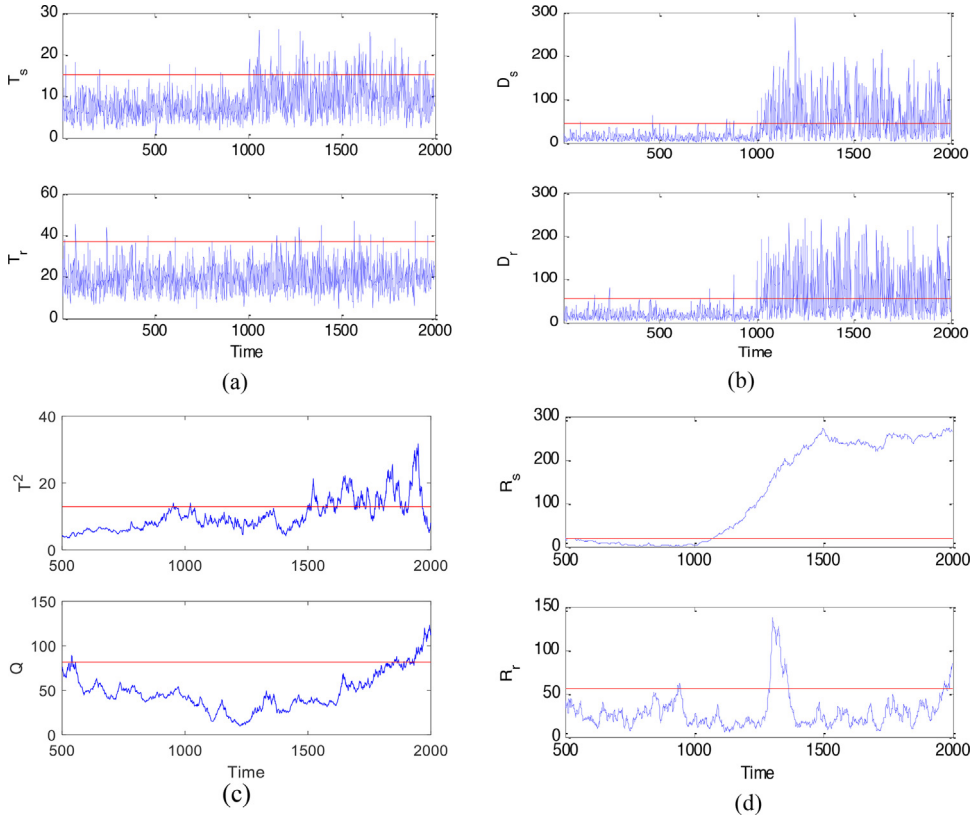

Fig. 4. Multivariate statistics for the detection for Fault GN1 with the fault magnitude $\delta = 1.6$ for (a) variable-based, (b) CD-based, (c) SPA-based, and (d) canonical correlation-based methods.

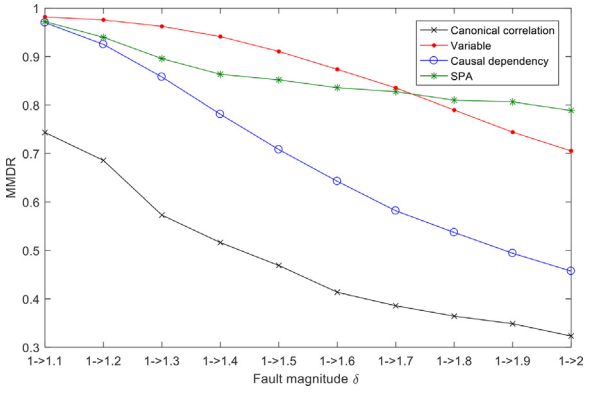

Fig. 5. The mean missed detection rate as a function of the fault magnitude for Fault GN2 ($\delta = 1$ under NOC). The methods in the legend are: Canonical correlation (i.e., the proposed canonical correlation-based method), Causal dependency (i.e., perform CVA on the CDs [29]), Variable (i.e., directly perform CVA on the process variables [29]), and SPA (i.e., perform DPCA on the statistics patterns [31]) methods. The notations $1 -> i$ in the horizontal coordinate means the fault magnitude δ linearly increases from $\delta = 1$ to $\delta = i$ during samples 1001–2000. For each method, a fault was indicated if either the state or residual statistic violated threshold.

aforementioned discussions, which are that (*i*) the deviations in the process correlation structures can be more effectively captured by the canonical correlation-based features; and (*ii*) the improved monitoring performance results from the less redundancy of the canonical correlation-based feature representation.

Likewise, Fig. 6 shows that the combined utilization of the state and residual statistics R_s and R_r for the canonical correlation-based method more persistently reveals a fault compared to the other methods, particularly with the fault magnitude for small values of δ (for the samples 1001–1500).

In this case study, the proposed canonical correlation-based approach was more effective for detecting both step-change (abrupt) and slow-drift (incipient) faults.

In addition, the false alarm rates for all the four methods are computed using an independent testing dataset with 2000 normal operating observations. The false alarm rates are tabulated in Table 2. The false alarm rate for the proposed canonical correlation-based method is comparable to the other methods.

5. Conclusions

This article presents a CVA-based canonical correlation approach for detecting changes in process dynamic correlations.

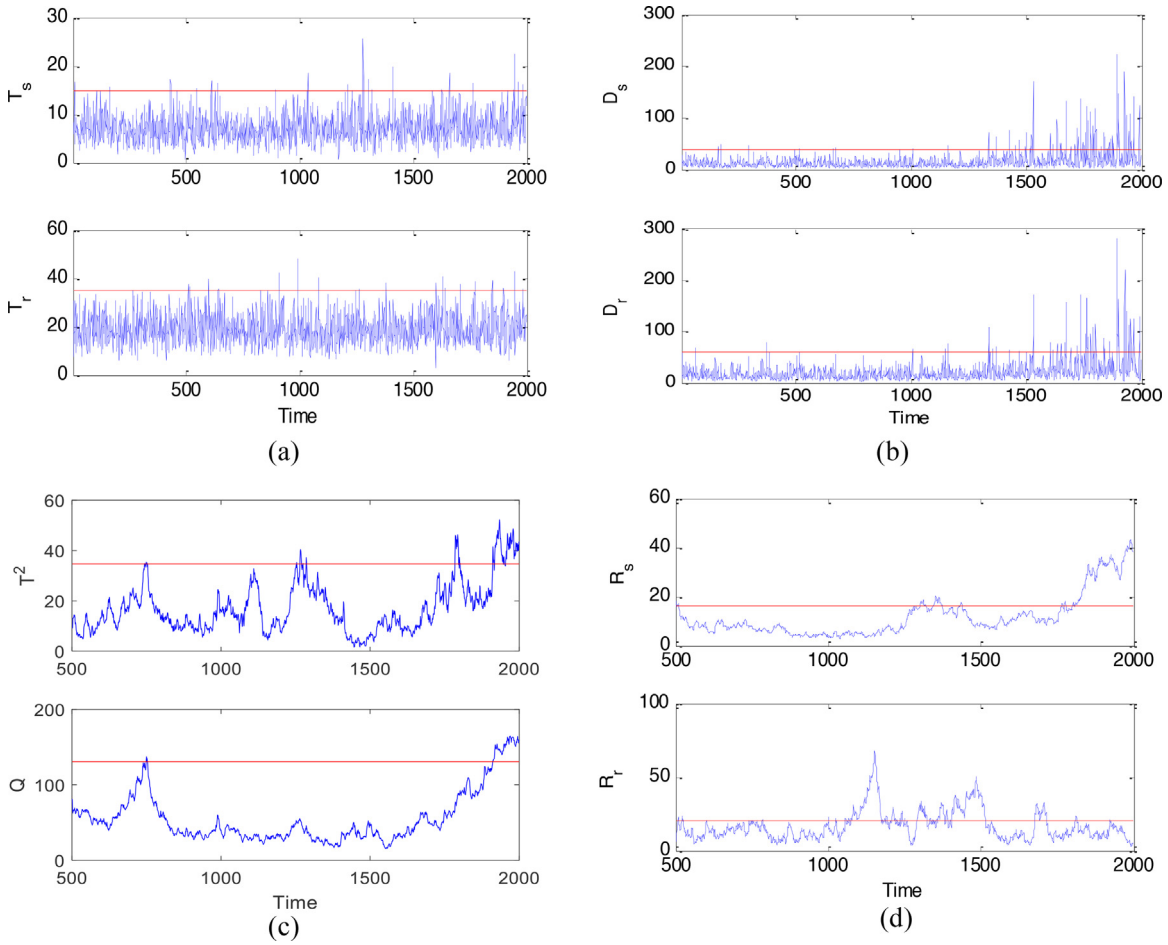

Fig. 6. Multivariate statistics for the detection for Fault GN2 with the fault magnitude δ linearly increases from $\delta = 1$ to $\delta = 1.3$ during the samples 1001–2000, for (a) variable-based, (b) CD-based, (c) SPA-based, and (d) canonical correlation-based methods.

Table 2
False alarm rates for the variable-based, CD-based, SPA-based and canonical correlation-based methods. For each method, a fault was indicated if either the state or residual statistic violated threshold.

Method	variable	CD	SPA	canonical correlation
False alarm rate	1.5%	2.7%	1.9%	2.2%

Two new statistics R_S and R_r are proposed that correspond to the state and residual spaces, respectively. The proficiency of fault detection is improved by employing canonical correlation features which provides more effective feature representation of the process compared with the original data, as well as a decreased degree of redundancy in the feature space. In the case studies of a gene network, the proposed canonical correlation-based method is significantly more effective for the cases of both step change and slow drift faults for the gene network model, with typical reduction in mean missed detection rate of a factor of 1.5–10.

The proposed method uses a moving window to calculate canonical correlations, which can be computationally expensive for some online fault detection applications. The online cost can be reduced by employing the fast moving window technique in [33]. The sensitivity for spike detection and detection delay for the proposed method depends on the size of moving window chosen in the singular value decomposition step (3). A smaller moving window number results in a smaller detection delay and higher detection sensitivity for spikes and vice versa. However, a smaller window size also leads to lower accuracy of the canonical correlations. The selection of window size depends on the specific need for an industrial process. When the promptness of fault detection is of high demand, a small window size should be used. A large window size should be adopted when the accuracy of fault detection is more important.

Acknowledgements

Dr. Xiaoxiang Zhu at MIT is appreciated for helpful discussions. Yi Luo at BUCT is appreciated for the help on simulations. This work is supported by the National Natural Science Foundation of China (61603024) and the High-Level Talents Fund of BUCT (buctrc201).

Appendix A.

Maximizing Mutual Information Viewpoint for the Optimality of CVA in Modeling

This section discusses how, in the Gaussian case, the objective of CVA on maximizing the correlation between the future and past variables is equivalent to maximizing the mutual information between these two sets of variables.

Consider the jointly distributed Gaussian random variables $\boldsymbol{p}$ and $\boldsymbol{f}$,

$$\begin{pmatrix} \boldsymbol{p} \\ \boldsymbol{f} \end{pmatrix} \sim N\left(\begin{pmatrix} \boldsymbol{\mu}_{\mathbf{p}} \\ \boldsymbol{\mu}_{\mathbf{f}} \end{pmatrix}, \begin{pmatrix} \boldsymbol{\Sigma}_{\mathbf{p}} & \boldsymbol{\Sigma}_{pf} \\ \boldsymbol{\Sigma}_{fp} & \boldsymbol{\Sigma}_{\mathbf{f}} \end{pmatrix} \right). \tag{16}$$

Shannon's mutual information between $\boldsymbol{p}$ and $\boldsymbol{f}$ is

$$I(\boldsymbol{p},\boldsymbol{f}) = \frac{1}{2}\log\left(\frac{|\boldsymbol{\Sigma_p}||\boldsymbol{\Sigma}_f|}{|\boldsymbol{\Sigma}_{[\boldsymbol{p},\boldsymbol{f}]}|}\right). \tag{17}$$

where $|\cdot|$ denotes the determination of a matrix. Then maximizing the mutual information (MMI) can be stated as the optimization,

$$\max_{\boldsymbol{w}} I(\boldsymbol{w}^{\mathrm{T}}\boldsymbol{p};\boldsymbol{f}) = \max_{\boldsymbol{w}}\frac{1}{2}\log\left(\frac{|\boldsymbol{w}^{\mathrm{T}}\boldsymbol{\Sigma_p}\boldsymbol{w}||\boldsymbol{\Sigma_f}|}{|\boldsymbol{\Sigma}_{[\boldsymbol{w}^{\boldsymbol{T}}\boldsymbol{p},\boldsymbol{f}]}|}\right), \tag{18}$$

which is equivalent to maximizing

$$\max_{\boldsymbol{w}}\frac{|\boldsymbol{w}^{\mathrm{T}}\boldsymbol{\Sigma_p}\boldsymbol{w}||\boldsymbol{\Sigma_f}|}{|\boldsymbol{\Sigma}_{[\boldsymbol{w}^{\boldsymbol{T}}\boldsymbol{p},\boldsymbol{f}]}|}. \tag{19}$$

Since the denominator in (19) can be re-expressed as

$$|\boldsymbol{\Sigma}_{[\boldsymbol{w}^{\mathrm{T}}\mathbf{p},\mathbf{f}]}| = |\boldsymbol{\Sigma}_{\mathbf{f}}|\cdot|\boldsymbol{w}^{\mathrm{T}}\boldsymbol{\Sigma}_{\mathbf{p}}\boldsymbol{w} - \boldsymbol{w}^{\mathrm{T}}\boldsymbol{\Sigma}_{pf}\boldsymbol{\Sigma}_{\mathbf{f}}^{-1}\boldsymbol{\Sigma}_{fp}\boldsymbol{w}|, \tag{20}$$

Eq. (19) is equivalent to

$$\max_{\boldsymbol{w}}\frac{\boldsymbol{w}^{\mathrm{T}}\boldsymbol{\Sigma}_{\boldsymbol{pf}}\boldsymbol{\Sigma}_{\boldsymbol{f}}^{-1}\boldsymbol{\Sigma}_{\boldsymbol{fp}}\boldsymbol{w}}{\boldsymbol{w}^{\mathrm{T}}\boldsymbol{\Sigma}_{p}\boldsymbol{w}} \tag{21}$$

which is equivalent to solving the generalized eigenvalue decomposition:

$$\boldsymbol{\Sigma}_{pf}\boldsymbol{\Sigma}_{\boldsymbol{f}}^{-1}\boldsymbol{\Sigma}_{\boldsymbol{fp}}\boldsymbol{w} = \lambda\boldsymbol{\Sigma}_{p}\boldsymbol{w}. \tag{22}$$

Eq. (22) yields the same solution as CVA. Therefore, maximizing the mutual information is the same as maximizing correlation in the Gaussian case. In addition, it was pointed out in [34] that the method that maximizes the mutual information between the predicting and predicted variables claims optimality in terms of minimizing the mean squared error (MSE) of the model for linear Markov systems. Thus, the objective of CVA on maximizing the correlation between the past and future variables is optimal in model performance, i.e., achieves the minimum error of model prediction.

Appendix B.

Physical Meaning for the Proposed Canonical Correlation-based Approach

The CVA optimization (1)–(2), which is solved via the singular value decomposition (SVD) of (3), can be equivalently computed by the generalized eigenvalue decomposition as [27]

$$\boldsymbol{\Sigma}_1\boldsymbol{v}_i = \lambda_i\boldsymbol{\Sigma}_2\boldsymbol{v}_i, \tag{23}$$

where $\boldsymbol{\Sigma}_1 = \begin{bmatrix}\mathbf{0} & \boldsymbol{\Sigma_{pf}}\\ \boldsymbol{\Sigma_{fp}} & \mathbf{0}\end{bmatrix}$, $\boldsymbol{\Sigma}_2 = \begin{bmatrix}\boldsymbol{\Sigma_{pp}} & \mathbf{0}\\ \mathbf{0} & \boldsymbol{\Sigma_{ff}}\end{bmatrix}$, $\boldsymbol{v}_i = \begin{bmatrix}\boldsymbol{J}_{(i)\mathrm{T}}\\ \boldsymbol{L}_{(i)\mathrm{T}}\end{bmatrix}$, and 0 is the matrix of zeros of compatible dimensions.

The generalized eigenvalue system (23) used in the solution of proposed CVA-based fault detection approach can be given a physical interpretation. A spring-mass system can be constructed by taking process variables as spring nodes and connecting each pair of process variables as springs connecting each pair of nodes. The correlation degree of each connective pair of nodes is defined as the spring stiffness, and the total degree of correlation connecting to a node is defined as its mass.

If a hard shake were given to this spring-mass system, nodes that have stronger spring connections among them would more likely oscillate together, which is analogous to the fact that faults would more likely transfer between the process variables that have stronger connections among them. As the shaking becomes more violent, the properties of process dynamic relations connecting to this group of nodes will be altered. The fundamental oscillation mode of the nodes can represent its overall steady-state behaviors. Actually, the generalized eigenvectors of (23) exactly describe the fundamental oscillation modes of the spring-mass system.

From [28,35], this spring-mass dynamical system can be represented by

$$\boldsymbol{M}(\ddot{\boldsymbol{x}})(t) = -\boldsymbol{K}\boldsymbol{x}(t), \tag{24}$$

where the diagonal matrix $\boldsymbol{M}\in R^{n\times n}$ is the mass matrix with $\boldsymbol{M}(i,i) = \sum_i \boldsymbol{k_{ij}}$, $\boldsymbol{x}(t)\in R^{n\times 1}$ denotes the vector describing the motion of each node, k_{ij} is the spring stiffness of the connecting nodes i and j, and $\boldsymbol{K}\in R^{n\times n}$ denotes the stiffness matrix with $\boldsymbol{K}(i,i) = \sum_i k_{ij}$ and $\boldsymbol{K}(i,j) = -k_{ij}$.

Given that the motion vector $\boldsymbol{x}(t)$ has the form of $\boldsymbol{x}(t) = \boldsymbol{v_i}\cos(\omega_i t + \theta)$, the solution for the steady-state behavior of the spring-mass system is [28,35]

$$\boldsymbol{K}\boldsymbol{v}_i = \omega_i^2\boldsymbol{M}\boldsymbol{v}_i, \tag{25}$$

which is analogous to (23) for the solution of proposed CVA-based fault detection approach.

The solutions $(\omega_i, \boldsymbol{v}_i)$ of (25) represent the fundamental modes of this spring-mass system. The eigenvectors v_i show the steady-state movement of each mode of oscillation and the eigenvalues ω_i^2 indicate the energy required to sustain the oscillation modes [35]. Similarly, the solution pairs $(\lambda_i, \boldsymbol{v}_i)$ of (23) describe the fundamental modes of a process dynamic system. The eigenvectors $\boldsymbol{v}_i$ show the steady-state behavior of the dynamic relations in each mode. The eigenvalues λ_i indicate the energy that each dynamic mode owns, which is consistent with the viewpoint in [27] that calculating canonical correlations via CVA leads to a maximization of the energy λ_i.

References

[1] L.H. Chiang, B. Jiang, X. Zhu, D. Huang, R.D. Braatz, Diagnosis of multiple and unknown faults using the causal map and multivariate statistics, J. Process Control 28 (2015) 27–39.
[2] H. Hotelling, The generalization of student's ratio, Ann. Math. Stat. 2 (1931) 360–378.
[3] A. Negiz, A. Çinar, Statistical monitoring of multivariable dynamic processes with state-space models, AIChE J. 43 (1997) 2002–2020.
[4] A. Negiz, A. Çinar, PLS, balanced, and canonical variate realization techniques for identifying VARMA models in state space, Chemometr. Intell. Lab. Syst. 38 (1997) 209–221.
[5] A. Prieto-Moreno, O. Llanes-Santiago, E. García-Moreno, Principal components selection for dimensionality reduction using discriminant information applied to fault diagnosis, J. Process Control 33 (2015) 14–24.
[6] S. Yin, S.X. Ding, A. Haghani, H. Hao, P. Zhang, A comparison study of basic data-driven fault diagnosis and process monitoring methods on the benchmark Tennessee Eastman process, J. Process Control 22 (2012) 1567–1581.
[7] F. He, J. Xu, A novel process monitoring and fault detection approach based on statistics locality preserving projections, J. Process Control 37 (2016) 46–57.
[8] V.B. Ghute, D.T. Shirke, A multivariate synthetic control chart for process dispersion, Qual. T. Quant. Manage. 5 (2008) 271–288.
[9] L. Liu, J. Zhong, Y. Ma, A multivariate synthetic control chart for monitoring covariance matrix based on conditional entropy, in: E. Qi, J. Shen, R. Dou (Eds.), The 19th International Conference on Industrial Engineering and Engineering Management, Springer, Berlin, Heidelberg, 2013, pp. 99–107.
[10] V. Mayer-Schonberger, K. Cukier, Big Data: A Revolution That Will Transform How We Live Work and Think, John Murray Publishers, London, 2013.
[11] M.S. Sarfraz, O. Hellwich, Z. Riaz, Feature extraction and representation for face recognition, in: M. Oravec (Ed.), Face Recognition, InTech, Croatia, 2010, pp. 1–20.
[12] D. Garcia-Alvarez, M.J. Fuente, G.I. Sainz, Fault detection and isolation in transient states using principal component analysis, J. Process Control 22 (2012) 551–563.
[13] J.E. Jackson, G.S. Mudholkar, Control procedures for residuals associated with principal component analysis, Technometrics 21 (1979) 341–349.
[14] J.F. MacGregor, C. Jaeckle, C. Kiparissides, M. Koutoudi, Process monitoring and diagnosis by multiblock PLS methods, AIChE J. 40 (1994) 826–838.
[15] G. Li, S.J. Qin, D. Zhou, Geometric properties of partial least squares for process monitoring, Automatica 46 (2010) 204–210.
[16] B. Jiang, D. Huang, X. Zhu, F. Yang, R.D. Braatz, Canonical variate analysis-based contributions for fault identification, J. Process Control 26 (2015) 17–25.

[17] P.E.P. Odiowei, Y. Cao, Nonlinear dynamic process monitoring using canonical variate analysis and kernel density estimations, IEEE Trans. Ind. Inf. 6 (2010) 36–45.
[18] L.H. Chiang, E.L. Russell, R.D. Braatz, Fault Detection and Diagnosis in Industrial Systems, Springer Verlag, U. K, 2001.
[19] E.L. Russell, L.H. Chiang, R.D. Braatz, Fault detection in industrial processes using canonical variate analysis and dynamic principal component analysis, Chemometr. Intell. Lab. Syst. 51 (2000) 81–93.
[20] B. Jiang, X. Zhu, D. Huang, J.A. Paulson, R.D. Braatz, A combined canonical variate analysis and Fisher discriminant analysis (CVA–FDA) approach for fault diagnosis, Comput. Chem. Eng. 77 (2015) 1–9.
[21] A. Simoglou, E.B. Martin, A.J. Morris, Statistical performance monitoring of dynamic multivariate processes using state space modelling, Comput. Chem. Eng. 26 (2002) 909–920.
[22] T.W. Anderson, An Introduction to Multivariate Statistical Analysis, 3rd ed., Wiley, New Jersey, 2003.
[23] H. Akaike, A new look at the statistical model identification, IEEE Trans. Autom. Control 19 (1974) 267–281.
[24] H. Akaike, Markovian representation of stochastic processes by canonical variables, SIAM J. Control 13 (1975) 162–173.
[25] W.E. Larimore, Canonical variate analysis in control and signal processing, in: T. Katayama, S. Sugimoto (Eds.), Statistical Methods in Control and Signal Processing, Marcel Dekker Inc., New York, 1997, pp. 83–120.
[26] S.J. Qin, Statistical process monitoring: basics and beyond, J. Chemometr. 17 (2003) 480–502.
[27] M. Borga, T. Landelius, H. Knutsson, A unified approach to PCA, PLS, MLR and CCA. Report LiTH-ISY-R-1992, Linköping, Sweden, November 1997.
[28] J.G. Fox, J. Mahanty, The effective mass of an oscillating spring, Am. J. Phys. 38 (1970) 98–100.
[29] B. Jiang, X. Zhu, D. Huang, R.D. Braatz, Canonical variate analysis-based monitoring of process correlation structure using causal feature representation, J. Process Control 32 (2015) 109–116.
[30] Y. Tamada, S. Kim, H. Bannai, S. Imoto, K. Tashiro, S. Kuhara, S. Miyano, Estimating gene networks from gene expression data by combining Bayesian network model with promoter element detection, Bioinformatics 19 (2003) ii227–ii236.
[31] J. Wang, Q.P. He, Multivariate statistical process monitoring based on statistics pattern analysis, Ind. Eng. Chem. Res. 49 (2010) 7858–7869.
[32] G. Li, S.J. Qin, Comparative study on monitoring schemes for non-Gaussian distributed processes, J. Process Control (2016), http://dx.doi.org/10.1016/j.jprocont.2016.08.007.
[33] X. Wang, U. Kruger, G.W. Irwin, Process monitoring approach using fast moving window PCA, Ind. Eng. Chem. Res. 44 (2005) 5691–5702.
[34] J. Galdos, D. Gustafson, Information and distortion in reduced-order filter design, IEEE Trans. Inf. Theory 23 (1977) 183–194.
[35] J. Shi, J. Malik, Normalized cuts and image segmentation, IEEE Trans. Pattern Anal. Mach. Intell. 22 (2000) 888–905.